Journal of Solid State Chemistry **164,** 169–175 (2002)
doi:10.1006/jssc.2001.9470, available online at http://www.idealibrary.com on IDEAL®

Synthesis and Crystal Structure of $M_{11}X_{10}$ Compounds, M = Sr, Ba and X = Bi, Sb. Electronic Requirements and Chemical Bonding

Gaëlle Derrien, Monique Tillard-Charbonnel,[1] Alain Manteghetti, Laure Monconduit, and Claude Belin

Laboratoire des Agrégats Moléculaires et Matériaux Inorganiques UMR CNRS 5072, Université de Montpellier II, Sciences et Techniques du Languedoc, Place Eugène Bataillon, 34095 Montpellier Cédex 5, France

Received July 24, 2001; in revised form November 13, 2001; accepted November 30, 2001

The intermetallic compounds $Sr_{11}Bi_{10}$, $Ba_{11}Bi_{10}$, and $(Sr_5Ba_6)Sb_{10}$ have been obtained from melts of mixtures of the elements. They crystallize in the tetragonal system, space group $I4/mmm$, $Ho_{11}Ge_{10}$ structure type, tI84 Pearson symbol, $Z = 4$, with cell parameters $a = 12.765(3)$, 13.230(3), 12.748(2) Å and $c = 18.407(3)$, 19.365(3), 18.761(2) Å, respectively. The structures were solved from single-crystal X-ray data and refined by full-matrix least-squares to $R1 = 6.71$, 5.44, and 5.73%. The structure of $M_{11}X_{10}$ contains three discrete anionic moieties: square rings X_4^{4-}, dumbbells X_2^{4-}, and isolated X^{3-}. Using formal charges the unit cell of $M_{11}X_{10}$ may be described as containing 44 M^{2+}, 2X_4^{4-}, 8X_2^{4-}, and 16X^{3-} ions. This structure is discussed in comparison with other Bi or Sb pnictide compounds. Bonding is analyzed therein using molecular orbital (EHMO) calculations for the anions (dumbbell and square units) and also the periodic tight-binding method. Lone pair repulsions inside and between the anionic units are evidenced; they are compensated by strong bonding cation-to-anion interactions. Interatomic distances along the series appear to be more dependent on packing than on electronic effects. © 2002 Elsevier Science (USA)

Key Words: **bismuthides; antimonides; pnictides; dumbbell; square ring; oligomeric anions.**

INTRODUCTION

The literature also contains several crystallographic results relative to bismuth and alkaline-earth metal systems. Compounds M_2X with M = Ca, Sr, Ba and X = Bi, As, Sb were found to be tetragonal (7–9) Compounds M_5Bi_3 with M = Ca, Sr, Ba have been the most studied: Ba_5Bi_3 (8, 10) was described as orthorhombic with the β-Yb_5Sb_3 structure-type and Ca_5Bi_3 hexagonal (11) with the Mn_5Si_3 structure-type. The isostoichiometric compound Sr_5Bi_3 displays the two crystallographic hexagonal (8) and orthorhombic (10) structures. The study of compounds M_5X_3, M = Ca, Sr, Ba and X = Bi, Sb, and their reactivity toward halogens and sulfur (12) was carried out later. The authors stress the role of size tuning between elements in the adoption of one or the other of the two crystallographic forms. In all the aforementioned compounds, Bi atoms are isolated and exclusively surrounded by alkali or alkaline-earth atoms in their first coordination shell. On the electronic point of view, the M_5X_3 phases cannot be described by considering only X^{3-} units. In $Ca_{11}Bi_{10}$ (13) there are monoatomic anions but also oligomeric anions: Bi_2 dumbbells and Bi_4 square planar rings. From X-ray powder data, $Sr_{11}Bi_{10}$ had been found to be isotypic (14). Sr_2Bi_3 displays an original structure in which 2- and 3-connected Bi atoms form slabs (14).

Lots of alkali or alkaline-earth metal antimonide compounds contain only monoatomic anions. This is the case for Li_3Sb, Na_3Sb, K_3Sb (3), Ba_2Sb (8), Ca_2Sb (15), Sr_2Sb (16), Ba_5Sb_3 (8, 12), Ca_5Sb_3 (9, 17), Sr_5Sb_3 (18), and $Ca_{16}Sb_{11}$ (19). Recent work has shown the orthorhombic M_5X_3 compounds to incorporate interstitial hydrogen; particularly Ca_5Sb_3 has been reformulated Ca_5Sb_3H (20). In its two crystallographic forms, Ba_5Sb_4 contains two anionic species, Sb^{3-} and Sb_2^{4-} (21, 22), while three anionic species (isolated Sb atoms, Sb_2 dumbbells, and Sb_4 square planar rings) coexist in $Ca_{11}Sb_{10}$ (13) and $Sr_{11}Sb_{10}$ (23). In contrast to bismuthides, antimonides display a richer variety of anionic arrangements (24). Li_2Sb contains Sb_2 dumbbells and Sb_n infinite linear chains (25, 26) and K_5Sb_4 is described with discrete units labeled Sb_4^{5-} (27). A more recent work (28) that reports on metallic salts M_5X_4 (M = K, Rb, Cs; X = As, As, Bi) claims that these compounds contain zig-zag X_4^{4-} tetramers and an extra delocalized electron. Discrete anions Sb_7^{3-} and Sb_2^{4-}, respectively, have been found recently in compounds Cs_3Sb_7 and Cs_4Sb_2 (29). Zigzag planar infinite chains form in $CaSb_2$ (30) or $SrSb_2$ (31) and Te-like infinite chains in MSb compounds (M = Na, K, Rb, Cs) (32–34). In compound KSb_2, Sb atoms form hexagonal puckered rings condensed into one-dimensional chains

[1]To whom correspondence should be addressed. E-mail: mtillard@univ-montp2.fr. Fax: (33) 04 67 14 33 04.

0022-4596/02 $35.00

(35). Two-dimensional $[Sb_3^{2-}]$ networks are observed in $BaSb_3$ (36) and Ba_2Sb_3 (37) contains hexagon-based helicoidal chains that are interconnected to form a three-dimensional framework of the Sr_2Sb_3 type (38).

This paper will report syntheses and crystal structures of three compounds containing bismuth or antimony isolated atoms, dimers, and tetramers. They are compared with isostructural $Ca_{11}Bi_{10}$, $Ca_{11}Sb_{10}$ (13), and $Sr_{11}Sb_{10}$ (23). Bonding therein will be analyzed on the basis of molecular and three-dimensional extended Hückel calculations.

EXPERIMENTAL SECTION

Elements used were barium (Merck, 99%), strontium (Aldrich, 99%), antimony (Merck, 99.8%), and bismuth (Fluka, 99.99%). The Sr:Bi and Ba:Bi mixtures were prepared in the stoichiometric ratio 5/4, and the Sr:Ba:Sb in proportions 2.5/2.5/4. The mixtures were enclosed in tantalum reactors, weld-sealed under an argon atmosphere, and protected from oxidation by evacuated silica jackets. The mixtures were heated to 1373 K for 10 hours, and then kept at 1223 K for 100 hours, and finally cooled to room temperature at the rate of 150° per hour. The fairly homogeneous products of the reactions, being sensitive to air, were handled in a glove box filled with purified argon. Microprobe analyses of several single crystals indicated the absence of Ta contaminant. *M*/Bi ratios of approximately 1.12(2)/1 and a Sr/Ba/Sb ratio of nearly 0.49(1)/0.62(1)/1 were found. Small crystalline pieces were selected under a microscope in the glove box and mounted into Lindemann glass capillaries to be checked for singularity by preliminary oscillation and Weissenberg diffraction techniques. For each compound, the best diffracting crystal was chosen for data collection at room temperature on an Enraf Nonius CAD-4 automatic diffractometer, Mo$K\alpha$ radiation ($\lambda = 0.71069$ Å). Accurate lattice parameters were determined by least-squares refinement of the angular positions of 25 collected reflections automatically centered on the diffractometer. Three standard reflections were checked after every 100 reflections without any significant loss in intensities. Data were first corrected for background and Lorentz-polarization effects. Once the exact composition of the crystals was known, a numerical absorption correction was applied using the procedure provided by SHELX76 (39). Structures were solved by the direct methods of the SHELXS97 program (40) and refined by the full-matrix least-squares procedure of SHELXL97 (41). Anisotropic thermal parameters were used for all atoms in final refinements. A summary of crystallographic data for all compounds is given in Table 1. Atomic coordinates and displacement parameters are given in Table 2 and main bond distances in Table 3.

TABLE 1
Summary of Crystallographic Data

	$Sr_{11}Bi_{10}$	$Ba_{11}Bi_{10}$	$Sr_{5.2}Ba_{5.8}Sb_{10}$
Formula weight, Z	3053.6, 4	3600.5, 4	2386.1, 4
Space group		*I*4/*mmm*, No. 139	
Cell parameters *a*, *c* (Å)	12.765(3), 18.407(3)	13.230(3), 19.365(3)	12.748(2), 18.761(2)
Volume (Å^3)	2999(1)	3389(1)	3049(1)
F(000)	4992	5784	4126
μ (mm^{-1})	77.77	64.22	25.06
Measured reflections (non zero)	2419 (1649)	2682 (1857)	2472 (1564)
R_{int} ($I > 2\sigma(I)$) (%)	6.80	5.90	5.70
Unique reflections	1064	1198	1009
Observed reflections ($I > 2\sigma(I)$)	572	678	564
Refined parameters	39	39	44
Weighting scheme	$1/[\sigma^2(Fo^2) + (0.060P)^2$	$1/[\sigma^2(Fo^2) + (0.031P)^2$	$1/[\sigma^2(Fo^2) + (0.029P)^2$
*R*1 (all)	0.1710	0.1502	0.1554
*R*1 ($I > 2\sigma(I)$)	0.0671	0.0544	0.0573
w*R*2 (all)	0.1681	0.1338	0.1250
w*R*2 ($I > 2\sigma(I)$)	0.1410	0.1127	0.1049
Goodness of fit	0.964	1.028	1.037
ρ_{max} (e.Å^{-3})	4.24	4.57	2.24
ρ_{min} (e.Å^{-3})	− 4.28	− 3.96	− 2.90

$Sr_{11}Bi_{10}$. The crystal was shiny dark with dimensions $0.12 \times 0.09 \times 0.08$ mm. Intensities were collected within the octant *hkl* (*hkl* limits 0/12, 0/17, 0/25) of the *I*-tetragonal cell ($a = b = 12.765(3)$, $c = 18.407(3)$ Å). A total of 2419 reflections were measured in the range $2 < \theta < 30°$ with ω–θ scans. After the absorption effects were corrected ($\mu = 77.77$ mm^{-1}, transmission factor ranging from 0.032 to 0.209), the final refinement using 572 unique reflections with $I > 2\sigma(I)$ led to the agreement factors $R1 = 6.71$ and w$R2 = 14.10\%$.

$Ba_{11}Bi_{10}$. The crystal was a shiny dark platelet of dimensions $0.105 \times 0.060 \times 0.025$ mm. In order to provide for all contingencies in the structure analysis, reflection data were recorded within the octant *hkl* (*hkl* limits 0/26, 0/26, 0/27) of the *F*-centered orthorhombic cell ($a = 18.702(6)$, $b = 18.719(2)$, $c = 19.365(3)$ Å). Profile analysis of a few angle reflections indicated that ω–$1/3\theta$ scans were the most appropriate. A total of 2682 reflections were measured in the range $2 < \theta < 30°$. Data were corrected for absorption ($\mu = 64.22$ mm^{-1}, transmission factor ranging from 0.036 to 0.250). Checking the intensities indicated the crystal to really belong to the 4/*mmm* Laue class. Consequently, the cell was transformed into the *I*-tetragonal one ($a = b = 13.230(3)$, $c = 19.365(3)$ Å), the transformation matrix being $[\frac{1}{2}\ \frac{1}{2}\ 0,\ -\frac{1}{2}\ \frac{1}{2}\ 0,\ 0\ 0\ 1]$. Final refinement with 678 unique reflections having $I > 2\sigma(I)$ led to agreement factors $R1 = 5.44$ and w$R2 = 11.27\%$.

$Sr_{5.2}Ba_{5.8}Sb_{10}$. The relatively homogeneous product of the reaction displayed a silver luster. A triangular plate of

TABLE 2
Atomic Coordinates ($\times 10^4$) and Equivalent Isotropic Displacement Parameters ($Å^2 \times 10^3$)

Atom	Site	x	y	z	U_{eq}[a]
			$Sr_{11}Bi_{10}$		
Bi(1)	4*d*	5000	0	2500	11(1)
Bi(2)	4*e*	0	0	1277(2)	12(1)
Bi(3)	16*m*	2062(1)	2062(1)	3252(1)	14(1)
Bi(4)	8*i*	3487(2)	0	0	16(1)
Bi(5)	8*h*	1282(2)	1282(2)	5000	33(1)
Sr(1)	16*n*	2509(4)	0	1898(2)	18(1)
Sr(2)	4*e*	0	0	3408(5)	19(2)
Sr(3)	16*n*	5000	1616(4)	1027(2)	14(1)
Sr(4)	8*h*	1656(5)	1656(5)	0	34(2)
			$Ba_{11}Bi_{10}$		
Bi(1)		5000	0	2500	19(1)
Bi(2)		0	0	1201(2)	25(1)
Bi(3)		2102(1)	2102(1)	3217(1)	24(1)
Bi(4)		3565(2)	0	0	31(1)
Bi(5)		1242(2)	1242(2)	5000	50(1)
Ba(1)		2506(2)	0	1911(1)	25(1)
Ba(2)		0	0	3475(2)	26(1)
Ba(3)		5000	1680(2)	1032(1)	26(1)
Ba(4)		1695(2)	1695(2)	0	35(1)
			$Sr_5Ba_6Sb_{10}$		
Atom	sof	x	y	z	U_{eq}[a]
Sb(1)	0.125	5000	0	2500	17(1)
Sb(2)	0.125	0	0	1184(2)	30(1)
Sb(3)	0.5	2112(1)	2112(1)	3194(1)	19(1)
Sb(4)	0.25	3615(3)	0	0	42(1)
Sb(5)	0.5	1195(2)	1195(2)	5000	57(1)
Ba(1)	0.358(9)	2512(1)	0	1891(1)	20(1)
Sr(1)	0.142(9)	2512(1)	0	1891(1)	20(1)
Ba(2)	0.125	0	0	3438(2)	20(1)
Ba(3)	0.077(9)	5000	1695(2)	1043(1)	25(1)
Sr(3)	0.423(9)	5000	1695(2)	1043(1)	25(1)
Ba(4)	0.157(7)	1733(2)	1733(2)	0	37(1)
Sr(4)	0.093(7)	1733(2)	1733(2)	0	37(1)

[a] $U_{eq} = [\sum_j \sum_j U_{ij} a_i^* a_j^* \bar{a}_i \bar{a}_j]]/3$. For $Sr_5Ba_6Sb_{10}$, the number of atoms in the unit cell is $32 \times$ sof.

dimensions $0.20 \times 0.05 \times 0.02$ mm was chosen for data collection. A total of 2472 reflections were measured within the octant *hkl* (*hkl* limits 0/12, 0/17, 0/26) of the *I*-centered tetragonal cell ($a = b = 12.748(2)$, $c = 18.761(2)$ Å) in the range $2 < \theta < 30°$ ($\omega - \theta$ scans). After data were corrected for absorption effects ($\mu = 25.06\ mm^{-1}$, transmission factor ranging from 0.470 to 0.660), refinements with 564 unique reflections having $I > 2\sigma(I)$ were carried out to agreement factors $R1 = 5.73$ and w$R2 = 12.50\%$.

For all compounds, last Fourier differences indicated that the highest residual peaks in electron density occur in the near vicinity of the heavy atoms. We observed the same anomalies as reported in the literature for numerous representatives of the $Ho_{11}Ge_{10}$ structure type (42), i.e., fairly large atomic displacement parameters for atom *X*(5) at square unit and its *M*(4) neighbor that are located at 8*h* special position in the basal plane *x*, *x*, 0.

For compound $Sr_{11}Sb_{10}$ which we have also prepared, results (not reported here) are similar to those already published (23). These anomalous features are more marked for $Sr_{11}Sb_{10}$ and $Yb_{11}Sb_{10}$ (43). Our refinements of the $Sr_{11}Sb_{10}$ structure, even in lower symmetry space groups orthorhombic or monoclinic, did not clarify the problem. Varying the site occupation factors of *X*(5) and *M*(4) still led to values close to unity (full occupation), within standard deviation limits, and large atomic displacement parameters.

RESULTS AND DISCUSSION

The structures of $Sr_{11}Bi_{10}$, $Ba_{11}Bi_{10}$ and $Sr_{5.2}Ba_{5.8}Sb_{10}$ contain three discrete anion types: isolated Bi^{3-} (or Sb^{3-}), dumbbells Bi_2^{4-} (or Sb_2^{4-}) and square planar rings Bi_4^{4-} (or Sb_4^{4-}). A representation of the unit cell ($Z = 4$) is given in Fig. 1. These anions are separated by Ba^{2+} or Sr^{2+} cations. According to formal charges, a unit cell of $M_{11}X_{10}$ (M = Ba, Sr; X = Bi, Sb) is formulated: $44M^{2+}$, $2X_4^{4-}$, $8X_2^{4-}$, and $16X^{3-}$. In the compound $Sr_{5.2}Ba_{5.8}Sb_{11}$, Sr and Ba are disordered on cationic sites leading to a partition of the 44 cations into 23 Ba^{2+} and 21 Sr^{2+}.

In compounds $M_{11}X_{10}$ (X = Bi, Sb), the isolated anions X^{3-}, labeled *X*(1), *X*(2) and *X*(4), are surrounded in their first coordination shell by eight M^{2+} cations. Atom *X*(3) sits at the center of a capped trigonal prism of alkaline-earth atoms. Each prism shares a rectangular face with a neighbor, and two atoms *X*(3) are bonded to form anionic dimers Bi_2^{4-} or Sb_2^{4-}. Each *X*(5) atom is surrounded by seven alkaline-earth atoms and bonded to two alike atoms to form planar tetrameric anions Bi_4^{4-} or Sb_4^{4-}. In compound $Sr_{5.2}Ba_{5.8}Sb_{11}$, alkaline-earth atoms are disordered on all cationic sites except the (0,0,*z*) one which is filled with barium exclusively.

TABLE 3
Main *X*–*X* and Shortest *M*–*X* Interatomic Distances (Å) in $M_{11}X_{10}$ Compounds

X = Bi or Sb	$Sr_{11}Bi_{10}$	$Ba_{11}Bi_{10}$	$Sr_5Ba_6Sb_{10}$
X(3)–*X*(3)	3.187(3)	3.152(3)	2.955(3)
X(5)–*X*(5)	3.274(5)	3.286(4)	3.047(5)
X(3)–*X*(5)	3.513(2)	3.809(2)	3.771(2)
X(4)–*X*(4)	3.862(6)	3.796(5)	3.531(8)
M(4)–*X*(4)	3.151(2)	3.339(2)	3.261(3)
M(3)–*X*(3)	3.397(3)	3.528(2)	3.408(2)
M(3)–X(4)	3.400(4)	3.541(2)	3.408(3)
M(3)–X(1)	3.407(4)	3.608(2)	3.484(2)

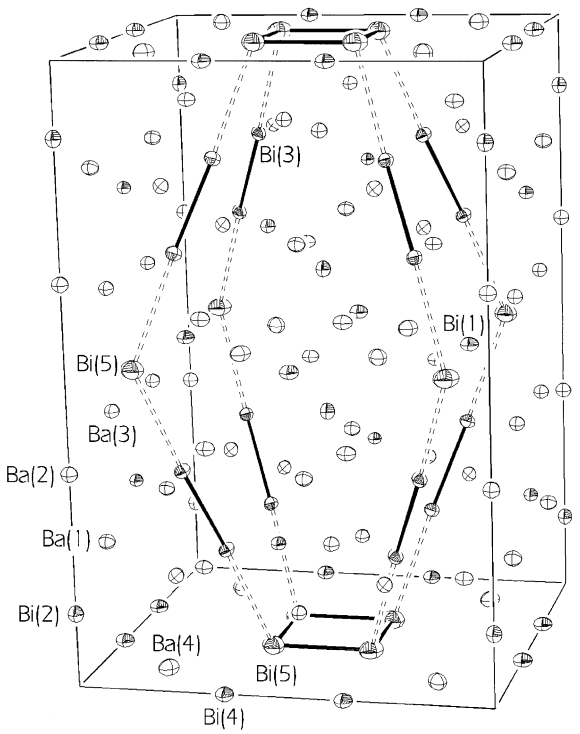

FIG. 1. Representation of the tetragonal unit cell of compound $Ba_{11}Bi_{10}$. Distances between dimers and tetramers are indicated as dashed lines.

In anionic units, Bi–Bi or Sb–Sb bond lengths range within the normal values for single bonds. Bi–Bi bond lengths are 3.274(5) and 3.286(4) Å in Bi_4^{4-} and 3.187(3) and 3.152(3) Å in Bi_2^{4-}, for $Sr_{11}Bi_{10}$ and $Ba_{11}Bi_{10}$, respectively. For comparison, Bi–Bi double bond lengths of 2.83 Å (44, 45) are reported in the literature for molecular compounds. A nearly square planar anion Bi_4^{2-} was reported (46), in which the Bi–Bi bond of 2.94 Å was intermediate between a single and double bond. Recently, a bond length of 2.976 Å (bond order higher than 1) has been found for a Bi_2 dumbbell in solid K_3Bi_2 (47). In Bi metal, Bi–Bi distances are 3.07 Å (48) and a single bond of 3.11 Å has been found for the Bi_2^{4-} dimer in KBa_4Bi_3O (49).

Similarly, interatomic distances of 2.955(3) Å in Sb_2^{4-} as well as 3.047(5) Å in Sb_4^{4-} for compound $Sr_{5.2}Ba_{5.8}Sb_{10}$ are also assigned to Sb–Sb single bonds (21, 22, 38, 50). They compare well with corresponding distances of 2.939(9) and 2.97(2) Å in $Sr_{11}Sb_{10}$ (23) and with reported distances of 2.923(2) Å for Sb_2 dumbbells in Cs_4Sb_2 (29). Interatomic distances of 2.91 Å (51) are found in Sb metal. Sb=Sb double bonds have shorter lengths ranging between 2.64 and 2.66 Å (44).

These bond lengths can also be compared with those reported for the isostructural $Ca_{11}Bi_{10}$ and $Ca_{11}Sb_{10}$ compounds (44). Noteworthy is the subsequent variation of some distances within the $M_{11}X_{10}$ series which deserves some analysis. Within dumbbells and square rings, intra-anionic distances are almost independent of the nature of the alkaline-earth metal. Bi–Bi bonds lengths in dimers Bi_2^{4-} are 3.15, 3.19, and 3.15 Å for $Ca_{11}Bi_{10}$, $Sr_{11}Bi_{10}$, and $Ba_{11}Bi_{10}$, respectively. The corresponding Bi–Bi bond lengths in Bi_4^{4-} rings are 3.20, 3.27, and 3.29 Å. For the antimony compounds $Ca_{11}Sb_{10}$, $Sr_{11}Sb_{10}$, and $Sr_{5.2}Ba_{5.8}Sb_{10}$, Sb–Sb bonds have a very narrow length range: 2.94–2.95 Å (Sb_2^{4-} dumbbell) and 2.97–3.05 Å (Sb_4^{4-} square ring).

Also informative is the evolution of distances $X(3)$–$X(5)$ between the dimeric and tetrameric anions as a function of the alkaline-earth element period. These are 3.336, 3.513(2), and 3.809(2) Å in $Ca_{11}Bi_{10}$, $Sr_{11}Bi_{10}$, and $Ba_{11}Bi_{10}$, respectively. In the antimonides, they range from 3.363 Å in $Ca_{11}Sb_{10}$ to 3.603(8) Å in $Sr_{11}Sb_{10}$ and 3.771(2) Å in $Sr_{5.2}Ba_{5.8}Sb_{10}$. Noteworthy is the closeness of linking distances between Bi_4^{4-} (or Sb_4^{4-}) and Bi_2^{4-} (or Sb_2^{4-}) anions and bond lengths within these anions in $Ca_{11}Bi_{10}$ (or $Ca_{11}Sb_{10}$). This raises the question of the bonding, nonbonding, or antibonding nature and degrees of these interactions.

BONDING ANALYSIS

In order to analyze bonding within the anions and linking between them, molecular orbital and periodic extended Hückel calculations were performed. These calculations used an effective Hamiltonian (52) of the extended Hückel type with H_{ii} and ξ parameters given below (53). Molecular orbital calculations provide an analysis of the stability of the different discrete anionic species. Structural packing and interactions between anions will be discussed on the basis of 3-D calculations. Overlap populations for different bonds will be compared with regard to the nature of the pnictogen element and to the influence and size of the alkaline-earth countercations.

Molecular calculations have been carried out for all discrete anions X_2^{4-} and X_4^{4-} contained in $M_{11}X_{10}$ (M = Ca, Sr, Ba; X = Sb, Bi). Since the results are very similar, only those relative to Bi are reported and compared with results obtained for some less reduced anions Bi_2^{2-} (45, 47) and Bi_4^{2-} (46).

In Fig. 2 are represented the energy diagrams versus the interatomic Bi–Bi distance (Walsh diagrams) for Bi_2^{2-} and Bi_2^{4-} dimers. The large HOMO–LUMO separation confirms the stability of the two anionic species. For 12 valence electrons (Bi_2^{2-}, open shell), the best energetic stability is found for a Bi–Bi distance of 2.84 Å, and for 14 valence electrons (Bi_2^{4-}, closed shell) the most favorable interatomic distance is found close to 3.2 Å. For both anions, the HOMO is degenerate (π_g) and corresponds to p_y,p_z nonbonding orbitals. Molecular orbital overlap populations (MOOP) indicate a strong antibonding character for the

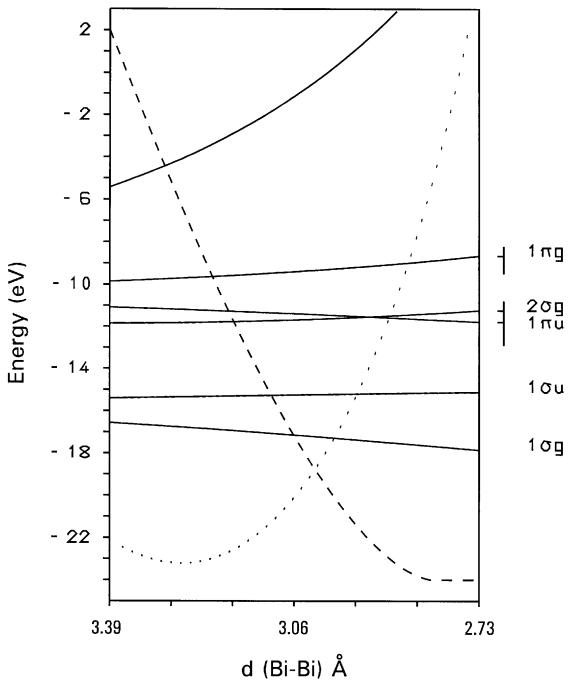

FIG. 2. Representation of Walsh diagrams for the diatomic anions Bi_2^{2-} and Bi_2^{4-} as a function of the interatomic distance between 2.73 and 3.39 Å. The sum of monoelectronic energies is represented as a dashed line for Bi_2^{2-} and a dotted line for Bi_2^{4-}.

HOMO (pair repulsions) leading to a bond order close to 1 for Bi_2^{4-}. When two valence electrons are removed (oxidation into Bi_2^{2-}) the global antibonding character is lowered and the bond order is raised to 2. These results are in agreement with the single bond length of 3.07 Å in Bi metal and with the Bi=Bi double bond lengths of 2.83 Å in molecular compounds (44, 45). Other Bi–Bi distances of 2.94 and 2.97 Å reported in square and dumbbell anions, respectively (46, 47), are halfway between a single and double bond.

In $M_{11}Bi_{10}$, Bi–Bi bonds of 3.28 Å are found within the tetra-atomic anion Bi_4^{4-} which displays the square planar D_{4h} geometry. According to Pauling's single bond radii for the elements (r_1(Bi) = 1.52 Å), these bonds would correspond to single bonds. The molecular orbital energy diagram for 24 electron filling shows a great separation HOMO (b_{2u})–LUMO (e_u), confirming the stability of the Bi_4^{4-} anion. A two-electron oxidation also leads to a significant HOMO (e_g)–LUMO (b_{2u}) separation and a good stability for the Bi_4^{2-} anion. Such an anion has been observed in the (crypt-K)$_2$Bi$_4$ compound (46) with a geometry slightly distorted from D_{4h}, and a Bi–Bi bond ($\sim$ 2.94 Å) intermediate between a single and double bond.

Three-dimensional electronic structures have been calculated for all the $M_{11}X_{10}$ (M = Ca, Sr, Ba; X = Sb, Bi) compounds. The results provide some new insights into the nature and strength of interactions between anions in these frameworks. Results are quite similar for bismuthides and antimonides, so only the case of $Ba_{11}Bi_{10}$ will be discussed here.

Total densities of states (DOS) and projected DOS for Ba and Bi atoms are shown in Fig. 3. Calculations have been carried out with a set of 64k points taken in the irreducible part of the Brillouin zone. Below the Fermi level ($-$ 4.4 eV, 288 electrons), the DOS exhibit two sets of bands with separated s ($-$ 18 to $-$ 13.6 eV) and p ($-$ 10.5 to $-$ 7 eV) contributions. It is noticeable that bands between $-$ 7 eV and Fermi energy (exclusively p in character) are dominated by Bi states. There is a good match between bismuth and barium states in the whole energy domain, indicative of some important covalent interactions.

Crystal orbital overlap populations (COOP) have been calculated for the different Bi-Bi bonds within oligomers and also for interactions between Bi atoms belonging to different units. They will provide informations about the nature (bonding, nonbonding or antibonding) and strength of interactions. Analysis of COOP curves, represented in Fig. 4, points out the strong antibonding character of some bands in the energy domain between $-$ 7.5 and $-$ 2 eV, on both sides of the Fermi level. These bands are assigned to interactions involving lone pairs at the bismuth atoms. Lone pair repulsions within the tetramer contribute in the bands at $-$ 4 and $-$ 2 eV and are partially compensated by bonding interactions involving Ba states. The band at $-$ 7.5 eV corresponds to similar lone pair repulsions within the dimer. The important antibonding contribution at $-$ 6 eV results from lone pair repulsions between anionic units (Bi^{3-} to Bi^{3-} and Bi_2^{4-} to Bi_4^{4-}). The tetrameric anion Bi_4^{4-} has a global bonding contribution up to an energy of $-$ 5 eV, yet the Bi_2^{4-} dimer displays antibonding at $-$ 7.5 eV. The strong bonding nature of the Ba–Bi

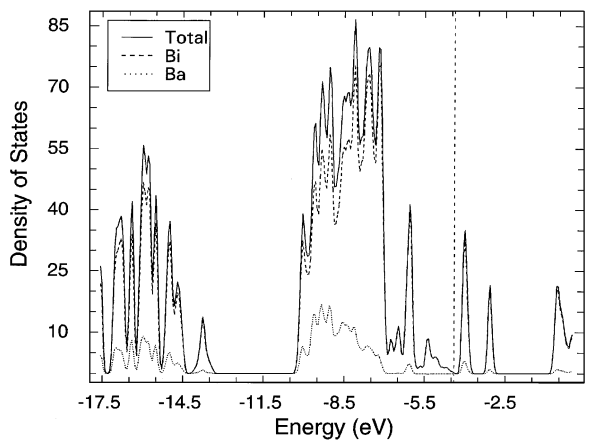

FIG. 3. Density of states (total DOS and atomic projections) for compound $Ba_{11}Bi_{10}$. The Fermi level has been represented at $-$ 4.4 eV for the unit cell electron content of 288 electrons.

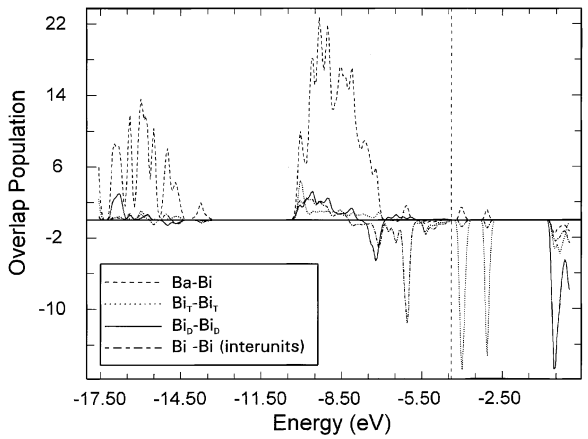

FIG. 4. Crystal orbital overlap populations (COOP) for different diatomic interactions in compound $Ba_{11}Bi_{10}$. The Fermi level has been represented at -4.4 eV for 288 electrons. Note that these different kinds of contacts (Ba–Bi and Bi–Bi) cannot be compared on the same scale.

interactions in the whole energy range under the Fermi level contributes to the stabilization of this ionocovalent structure.

In Table 4 are given the calculated overlap populations for atomic pairs within the oligomers and between them. Overlap populations have been calculated for distances up to 4.2 Å, so, in addition to bonding within the dimer (Bi_D–Bi_D) and within the tetramer (Bi_T–Bi_T), the interactions between two monomers (Bi_M–Bi_M) and between a dimer and a tetramer (Bi_D–Bi_T) are analyzed. As shown by the M–Bi overlap populations, interactions between alkaline-earth metal and bismuth display the same important bonding character over the $M_{11}Bi_{10}$ series.

While the Bi_M–Bi_M distance between two Bi^{3-} anions is fairly long (~ 3.8 Å) and remains almost unchanged, the antibonding overlap slightly increases from $Ca_{11}Bi_{10}$ to $Sr_{11}Bi_{10}$ and $Ba_{11}Bi_{10}$.

TABLE 4
Calculated Overlap Populations for Bonds in $M_{11}Bi_{10}$ Compounds for 288 Electrons (Fermi Level at -4.4 eV)

	$Ca_{11}Bi_{10}$		$Sr_{11}Bi_{10}$		$Ba_{11}Bi_{10}$	
	Overlap	d (Å)	Overlap	d (Å)	Overlap	d (Å)
Bi_D–Bi_D	0.24	3.15	0.32	3.19	0.43	3.15
Bi_T–Bi_T	0.33	3.20	0.36	3.27	0.43	3.29
Bi_D–Bi_T	0.03	3.33	-0.06	3.51	-0.09	3.81
Bi_M–Bi_M	-0.22	3.80	-0.25	3.86	-0.32	3.80
M–Bi	0.20	<4.20	0.20	<4.20	0.20	<4.20

[a] Bi atoms on tetramers and dimers are labeled Bi_T and Bi_D, respectively, and Bi_M stands for isolated Bi^{3-} anions.

The distances between Bi_2^{4-} and Bi_4^{4-} oligomeric anions increase along the series from 3.3 Å ($Ca_{11}Bi_{10}$) to 3.5 Å ($Sr_{11}Bi_{10}$) and 3.8 Å ($Ba_{11}Bi_{10}$). Owing to the small values of overlap populations (Bi_D–Bi_T), dimers and tetramers almost do not interact. Consequently, distances between dimers and tetramers do not depend upon electronic factors (polarization from alkaline-earth cations) but are rather ruled by the stacking mode (ionic radii are 1.75 Å for Ba^{2+}, 1.58 Å for Sr^{2+}, and 1.48 Å for Ca^{2+}).

Bi–Bi bond lengths within the dimer Bi_2^{4-} and the tetramer Bi_4^{4-} (Bi_D–Bi_D and Bi_T–Bi_T) do not vary significantly from $Ca_{11}Bi_{10}$ to $Ba_{11}Bi_{10}$; nevertheless, the corresponding overlap populations regularly increase. The progressive strengthening of these bonds is due to the decrease in electronegativities and the diminution of the polarization from cations along the series.

REFERENCES

1. E. Zintl and A. Z. Harder, *Phys. Chem.* **16B,** 206, 1932.
2. E. Zintl and G. Z. Brauer, *Electrokem. Angew. Phys. Chem.* **41**(5), 297 1935.
3. G. Brauer and E. Zintl, *Z. Phys. Chem.* **37B,** 323 (1937).
4. D. E. Sands, D. H. Wood, and W. J. Ramsey, *Acta Crystallogr.* **16,** 316 (1963).
5. N. N. Zhuravlev and V. P. Melik-Adamyan, *Sov. Phys. Crystallogr.* **6,** 99 (1961).
6. E. E. Havinga, H. Damsma, and M. H. van Maaren, *J. Phys. Chem. Solids* **31,** 2653 (1970).
7. B. Eisenmann and H. Schäfer, *Z. Naturforsch.* **29B,** 13 (1974).
8. B. Eisenmann and K. Deller *Z. Naturforsch.* **30B,** 66 (1975).
9. M. Martinez-Ripoll, A. Haase, and G. Brauer *Acta Crystallogr. B* **30,** 2003 (1974).
10. G. Bruzzone, E. Francesci, and F. Merlo, *J. Less Common Metals* **60,** 59 (1978).
11. M. Martinez-Ripoll, A. Haase, and G. Brauer, *Acta Crystallogr. B* **30,** 2004, (1974).
12. W. M. Hurng and J. D. Corbett, *Chem. Mater.* **1,** 311 (1989).
13. K. Deller and B. Eisenmann, *Z. Naturforsch.* **31B,** 29 (1976).
14. F. Merlo and M. Fornasini, *Mater. Res. Bull.* **29,** 149 (1994).
15. C. Hamon, R. Marchand, P. L'Haridon, and Y. Laurent *Acta Crystallogr. B* **31,** 427 (1975).
16. M. Martinez-Ripoll, A. Haase, and G. Brauer *Acta Crystllogr. B* **29,** 1715 (1973).
17. M. Martinez-Ripoll and G. Brauer *Acta Crystallogr. B* **30,** 1083 (1974).
18. M. Martinez-Ripoll, *Acta Crystallogr. B* **29,** 2717 (1973).
19. E. A. Leon Escamilla, W. M. Hurng, E. S. Peterson, and J. D. Corbett, *Inorg. Chem.* **36,** 703 (1997).
20. E. A. Leon Escamilla and J. D. Corbett, *J. Alloys Compds.* **206,** L15 (1994).
21. E. Brechtel, G. Cordier, and H. Schäfer, *Z. Naturforsch.* **36B,** 1341 (1981).
22. G. Derrien, L. Monconduit, M. Tillard, and C. Belin, *Acta Crystallogr. C* **55,** 1044 (1999).
23. A. Rehr and S. M. Kauzlarich, *Acta Crystallogr.* **50,** 1859 (1994).
24. G. A. Papoian and R. Hoffmann, *Angew. Chem. Int. Ed.* **39,** 2408 (2000).
25. R. Gerardin and J. Aubry, C. R., *Acad. Sci. Paris C* **278,** 1097 (1974).
26. W. Müller, *Z. Naturforsch.* **32B,** 357 (1977).
27. M. Somer, M. Hartweg, K. Peters, and H. G. von Schnering, *Z. Krist.* **103,** 195, (1991).
28. F. Gascoin and S. C. Sevov, *Inorg. Chem.* **40,** 5177 (2001).

29. C. Hirschle and C. Rhör, *Z. Anorg. Allg. Chem.* **626,** 1992 (2000).
30. K. Deller and B. Eisenmann, *Z. Anorg. Allg. Chem.* **425,** 104 (1976).
31. K. Deller and B. Eisenmann, *Z. Naturforsch.* **31B,** 1146 (1976).
32. D. T. Cromer, *Acta Crystallogr.* **12,** 41 (1959).
33. W. Hönle and H. G. von Schnering, *Z. Krist.* **155,** 307 (1981).
34. H. G. von Schnering, W. Hönle, and G. Krogull, *Z. Naturforsch.* **33B,** 1978 (1986).
35. A. Rehr, F. Guerra, S. Parkin, H. Hope, and S. M. Kauzlarich, *Inorg. Chem.* **34,** 6218 (1995).
36. K. Deller and B. Eisenmann, *Z. Naturforsch.* **33B,** 676 (1978).
37. B. Eisenmann, H. Jordan, and H. Schäfer, *Z. Naturforsch.* **40B,** 1603 (1985).
38. B. Eisenmann, *Z. Naturforsch.* **34B,** 1162 (1979).
39. G. M. Sheldrick, SHELX-76 Program for crystal structure determination, Univ. of Cambridge, England, 1976.
40. G. M. Sheldrick, SHELXS 97. A Program for Crystal Structures Solution, Univ. of Göttingen, Germany, 1997.
41. G. M. Sheldrick, SHELXL 97. A Program for Refining Crystal Structures, Univ. of Göttingen, Germany. 1997.
42. R. Schmelczer, D. Schwarzenbach, and F. Hulliger, *Z. Naturforsch.* **34B,** 1213 (1979).
43. H. L. Clark, H. D. Simpson, and H. Steinfink, *Inorg. Chem.*, **9/8,** 1962 (1968).
44. B. Twamley, C. D. Sofield, M. M. Olmstead, and P. P. Power, *J. Am. Chem. Soc.* **121,** 3357 (1999).
45. L. Xu, S. Bobev, J. El Bahraoui, and S. C. Sevov, *J. Am. Chem. Soc.* **122,** 1838 (2000).
46. A. Cisar and J. D. Corbett, *Inorg. Chem.* **16,** 2482 (1977).
47. F. Gascoin and S. C. Sevov, *J. Am. Chem. Soc.* **122,** 10251 (2000).
48. P. Cucka and C. S. Barret, *Acta Crystallogr.* **15,** 865 (1962).
49. G. Derrien, M. Tillard, L. Monconduit, and C. Belin, *Acta Crystallogr. C* **56,** 132 (2000)
50. G. Bolloré, M. J. Fergusson, R. W. Hushagen, and A. Mar, *Chem. Mater.* **7,** 2229 (1995).
51. C. S. Barrett, P. Cucka, and K. Haefner, *Acta Crystallogr.* **16,** 451 (1963).
52. R. Hoffmann, *J. Chem. Phys.* **39,**1397 (1963).
53. Parameters H_{ii} (eV) and Slater exponents ξ used in calculations: Sb, 5*s* − 18.8 and 2.323, 5*p* − 11.7 and 1.999; Bi, 6*s* − 15.19 and 2.56, 6*p* − 7.79 and 2.072; Ca, 4*s* − 6.111 and 1.2, 4*p* − 4.219 and 1.2; Sr, 5*s* − 6.62 and 1.214, 5*p* − 3.92 and 1.214; Ba, 6*s* − 6.32 and 1.23, 6*p* − 3.85 and 1.23.